Chapter 11

Quantum Computing with Atomic Qubits

11.1 Quantum Information and Qubits

Information science has led to big changes in our lives in the past seven decades since the first formulation of information theory by Claude Shannon. It is based on the quantification of information as the ability to distinguish different states. The basic unit of information is the binary digit, also known as the bit. It is the ability to distinguish between two states of 0 and 1, and has been the underlying principle for digital computation, information processing, and communication. However, all traditional information science is based on the classical physics of how the bit behaves: a given bit can take only one of the two available values at any given time in the middle of a computation or communication. A natural question arises: given that classical physics is a subset of quantum physics (or, quantum physics is a generalization of classical physics with correspondence principle that quantum physics reduces to classical physics in the "classical" limit), can we do more in information processing if we take advantage of quantum physics? The answer to this question turns out to be a resounding "YES", opening up a new field of quantum information science. In this Chapter, we discuss utilizing atoms for quantum computing. In the next Chapter, we will discuss utilizing atoms and photons for quantum communication.

The basic unit of quantum information is a quantum bit, or *qubit*. A qubit consists of two quantum states $|0\rangle$ and $|1\rangle$, each state representing the state of the information, similar to the bit in classical information processing. When the qubit is measured in the *comutational basis*, which means we ask the question "is the qubit in $|0\rangle$ state, or $|1\rangle$ state?", the qubit is projected into one of the two states corresponding to the two values of a classical bit (0 and 1), and corresponds to a classical bit. However, quantum bits are capable of so much more.

First, a qubit can be in an arbitrary linear superposition of the two qubit states, and is generally represented as

$$|\psi\rangle = \alpha |0\rangle + \beta |1\rangle = e^{i\gamma} \left[\cos\frac{\theta}{2} + e^{i\varphi}\sin\frac{\theta}{2}\right], \tag{11.1}$$

where the normalization condition $|\alpha|^2 + |\beta|^2 = 1$ allows one to represent the magnitude of the two coefficients as $\cos\theta/2$ and $\sin\theta/2$, respectively, with a phase difference φ between them. The overall phase γ is known as the global phase, and has no physical meaning whatsoever.

Second, in the presence of many qubits, qubits allow *entanglement* to be present, and used as a resource. Consider the state of two qubits, with four possible states $|00\rangle$, $|01\rangle$, $|10\rangle$ and $|11\rangle$, known as the computational basis states. A general quantum state allows an arbitrary superposition of these four states, as long as the square-sum of the coefficients adds up to one. For example, a state

$$|\psi_+\rangle = \frac{1}{\sqrt{2}}(|00\rangle + |11\rangle) \tag{11.2}$$

is an allowed state. This state, however, cannot be represented by describing the states of each qubit. For example, if one makes a measurement of the first qubit, it can result in both classical 0 and 1 states with equal probability. In that sense the first qubit is not in a well-defined state at all. The state of the second qubit is not independent of the first qubit at all: we see that while the measurement of the first qubit can yield a random result between 0 and 1, the successive measurement of the second qubit will result in exactly the same state as the result from the first qubit. This means that the state of the two qubits are intimately related, while the state of either qubit is determined independent of each other. The state in Eq. 11.2 cannot be expressed by a combination of an independent description of the two qubits. In fact, it is fully expressed by the correlation between the two states. This is an example of an entangled state, where the combined state of multiple qubits cannot be expressed by the combination of independent description of the component qubits. Furthermore, this state also is an example of a "maximally entangled state," where a maximum amount of entanglement exists between the two qubits. In a two-qubit case, there are four such maximally entangled states that are orthonormal and therefore forms an alternate basis set. The other three states are

$$|\psi_-\rangle = \frac{1}{\sqrt{2}}(|00\rangle - |11\rangle), \tag{11.3}$$

$$|\phi_+\rangle = \frac{1}{\sqrt{2}}(|01\rangle + |10\rangle), \tag{11.4}$$

$$|\phi_-\rangle = \frac{1}{\sqrt{2}}(|01\rangle - |10\rangle). \tag{11.5}$$

The power of quantum computation comes from the fact that when you have a n-qubit system, the general quantum state consists of a linear superposition of 2^n computational basis states. The number of the basis states grows exponentially, and a quantum state can in principle represent this exponentially large number of states simultaneously (or, represent the vast Hilbert space that these states live in). Nevertheless, it is important to know that when a measurement is made in the computational basis, only one of the component state is selected, with the probability given by the absolute value squared of the coefficient in front of this state in the superposition.

In order to realize a universal quantum computation, it is known that one must be able to (1) initialize the qubit to a fiducial start (often chosen to be $|0\rangle$ state), (2) reliably measure

the qubit between the $|0\rangle$ and the $|1\rangle$ state, and (3) apply a universal set of gates, often considered to be an arbitrary single qubit gate and at least one two-qubit gate that generated entanglement between two qubits. In this Chapter, we will discuss how such requirements can be met using atomic qubits.

11.2 Atomic Qubits

Just like classical bit that is always represented by a physical system with binary states (*e.g.*, a voltage state of a complementary metal-oxide-semiconductor, or CMOS, circuit in a digital processor, a magnetic domain in a hard disk drive, or an optical pulse in an optical communication system), a two-level quantum system must be used to represent a qubit. A good candidate physical system to represent the qubit must preserve the quantum state (both the amplitude θ and the relative phase ϕ in Eq. 11.1. It is important that the qubits can be obtained (or manufactured) reliably, with its properties being identical and reproducible. Individual atoms are great candidates for a qubit, because every atom is identical and reproducible. The choice of the states to represent qubit is also very important. In this chapter, we will consider utilizing hyperfine ground states of an atom with nuclear spin of 1/2 as the qubit states. Just like in the example of a hydrogen atom, the ground states are split into a triplet (with $F = 1$) and a singlet state (with $F = 0$). The two states $|F = 1, m_F = 0\rangle$ and $|F = 0, m_F = 0\rangle$ are an ideal choice for the qubit in this case, as the spontaneous decay between these two states are completely negligible (for hydrogen atom, it has a lifetime of $\sim 3 \times 10^{15}$ sec $= 10^7$ years), and the frequency difference is very stable against external electric and magnetic field fluctuations. Indeed, the hyperfine splitting of a Cs atom is used as a standard to **define** the absolute frequency reference. This means that the coherence time, the timescale over which the accuracy of the phase γ is lost, often due to the fluctuation of the frequency difference between the two qubit states, can be extended almost indefinitely in such a hyperfine qubit. These provide a strong advantage of the atomic hyperfine qubit over other fabricated qubits, such as a superconduting circuit qubit or a quantum dot qubit.

11.2.1 State initialization and detection

First, we consider how the qubit state can be initialized and measured. Figure 11.1 shows how optical pumping and resonance fluorescence processes can be used to achieve these functions. we consider the two hyperfine ground states to represent the qubit states $|0\rangle$ and $|1\rangle$. We consider two (types of) excited states $|e_0\rangle$ and $|e_1\rangle$. The first excited state(s) $|e_0\rangle$ is coupled to both ground states via dipole transition, *i.e.*, it decays to both ground states via spontaneous emission, and can therefore be excited from both states using a resonant laser beam with adequate polarization. On the other hand, the excited state $|e_1\rangle$ only couples to the $|1\rangle$ state via dipole transition. It only decays to $|1\rangle$ state through spontaneous emission, and decaly into the $|0\rangle$ state is forbidden by the atomic selection rules. There usually is a large enough energy splitting between the two qubit states (defined by the hyperfine splitting on the order of 1-20 GHz, much larger than the natural linewidths of the excited states determined by the spontaneous emission rate, on the order of 5-20 MHz), and the excitations can be turned on selectively by choice of the laser frequencies.
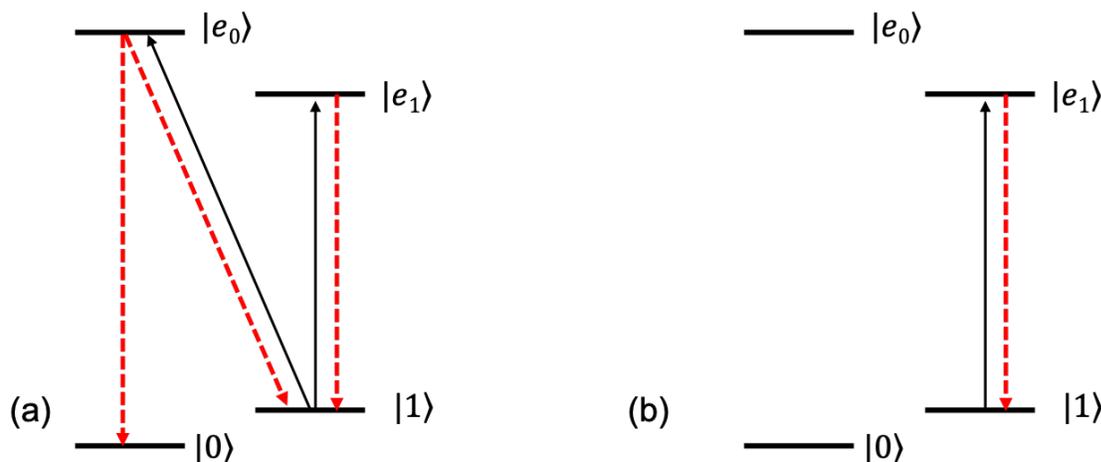
Figure 11.1: Simplified atomic level diagram to show schematic resonant processes for (a) qubit initialization and (b) qubit measurement process. The two states $|0\rangle$ and $|1\rangle$ denote the two hyperfine ground states used as a qubit. Two excited states are considered, $|e_0\rangle$ and $|e_1\rangle$, where $|e_0\rangle$ state is coupled to both $|0\rangle$ and $|1\rangle$ states via dipole transitions, while $|e_1\rangle$ state is only coupled to $|1\rangle$ state. Black solid lines show resonant laser beams for excitation, and the red dotted lines show spontaneous emission process. The $|e_1\rangle$ state only spontaneously decays to $|1\rangle$ state, while the $|e_0\rangle$ state can decay to both qubit states.

Figure 11.1(a) shows the initialization process via optical pumping. The excitation using narrow linewidth laser beam (narrower than the natural linewidth of the excited states) is shown in black arrows. The two frequencies excite $|1\rangle$ state to both excited states, which can decay into either the $|0\rangle$ state or back to the $|1\rangle$ state. After multiple excitation events, the electron will predominantly end up in the $|0\rangle$ state, initializing the qubit. In practice, the optical pumping can quickly prepare the atomic qubit in the $|0\rangle$ state with high purity: after scattering about 30 photons, the atom can be prepared in the $|0\rangle$ state with errors in the $\sim 10^{-6}$ range.

Figure 11.1(b) shows the qubit measurement process using state-dependent fluorescence process. In this case, a resonant laser beam that excites $|1\rangle$ state to the $|e_1\rangle$ state is turned on. If the electron is in the $|1\rangle$ state, the atom is excited to the $|e_1\rangle$ state, and emits a photon to decay back down to the $|1\rangle$ state. This process is repeated multiple times, and the atom continuously scatters photons, which can be detected by a sensitive photon detector (such as a single-photon detector). If the electron is in the $|0\rangle$ state, the excitation is off-resonant, and no photon scattering occurs. This is often referred to as the state-dependent fluorescence process where only one of the two states scatters photons. In practice, the two states can be differentiated with errors in the $< 10^{-3}$ range if a high numerical aperture optics is used to collect a good fraction of the scattered photons, and is detected with high-efficiency single

photon detectors with low background count levels.

11.2.2 Single qubit gates

Single qubit gate represents an arbitrary unitary operator that transforms the state of a single qubit state. Such a single qubit gate can be realized by driving resonant Rabi oscillations between the two qubit states, either using a resonant microwave field (similar to the magnetic resonant process considered in Section 3.2.3), or using two laser beams to drive a Raman transition as discussed in Section 10.1. By choosing the phase of the microwave field or the differential phase of the laser beams driving the Raman transition, and the duration of the field driving the Rabi oscillations, one can introduce an arbitrary unitary operators whose rotation angle and the phase of the rotation can be controlled. In practice, single qubit gates with errors in the $\sim 10^{-6}$ range have been demonstrated using microwave fields, and gates with errors in the $\sim 10^{-4}$ has been realized using Raman transitions. The errors for Raman transitions are often limited by the intensity noise and optical phase instability of the Raman beams at the location of the atomic qubit.

11.3 Entangling Gates in Atomic Qubits

The non-trivial quantum logic gate is the entangling gate. In order to generate entanglement, one must be able to change the state of one qubit based on the state of another qubit. Such qubit manipulation requires another physical degree-of-freedom that induces interaction between two atomic qubits. For neutral atoms, one can utilize the dipole-dipole interaction that can be induced by exciting a specific qubit state to a Rydberg state, where the atomic dopole moment can be increased by several orders of magnitude. One can also use atomic ions as qubits, where an electron is stripped from each atom, and the resulting ions are trapped tightly using electromagnetic trapping fields. In such an ion trap, the center-of-mass motion of the atomic ions in the trap is strongly coupled by the Coulomb interaction among the ions, and results in the normal modes of motion. These motional degrees of freedom can also function as a quantum system, and allow one to induce coupling by applying a state-dependent force.

The basic governing equation to describe ions coupled to a single normal mode of motion, driven by optical fields (such as Raman transitions for the case of hyperfine qubits) given by Eq. 8.53 in Section 8.3.2, with slightly different notations

$$\tilde{H}_I = \frac{\hbar}{2}\left(\Omega_0 e^{-i\eta_0(a^\dagger+a)}\left|0\right\rangle\left\langle 2\right| + \Omega_1 e^{-i\eta_1(a^\dagger+a)}\left|1\right\rangle\left\langle 2\right|\right) + h.c., \tag{11.6}$$

where Ω_0 and Ω_1 indicates the complex Rabi frequency of the transition (that includes the phase of the optical fields) driven between the $\left|0\right\rangle$ and $\left|1\right\rangle$ qubit states and the (virtual) excited state, respectively. After adiabatically eliminating the population of the excited state under large-detuning condition ($\Delta \gg \omega_{01} \gg \Gamma, \nu, \delta$, as in Eq. 8.46), the interaction Hamiltonian, after the light shift is accounted for, looks like

$$\hat{H}_I = \frac{\hbar\Omega}{2}e^{-i[(\Delta\delta+\delta)t+\eta(a^\dagger+a)]}\left|0\right\rangle\left|n\right\rangle_m\left\langle 1\right|\,_m\!\left\langle m\right| + h.c., \tag{11.7}$$

where $\Omega = \Omega_0 \Omega_1^* / (2\Delta$ is the effective Rabi frequency of the Raman transition and $\eta = \sqrt{\frac{\hbar}{2m\nu}}(\vec{k}_0 - \vec{k}_1) \cdot \hat{\varepsilon}_x$ is the effective Lamb-Dicke parameter arising from the difference of the momentum vectors of the two fields. By controlling the detuning of the Raman beams δ, one can drive either the carrier transition $|0\rangle |n\rangle_m \leftrightarrow |1\rangle |n\rangle_m$, the red-sideband transition $|0\rangle |n\rangle_m \leftrightarrow |1\rangle |n-1\rangle_m$, or the blue-sideband transition $|0\rangle |n\rangle_m \leftrightarrow |1\rangle |n+1\rangle_m$, where the change in the motional excitation for the shared normal mode is 0, -1 and +1, respectively.

We discuss two different schemes for realizing entangling gates in a trapped ion system.

11.3.1   Cirac-Zoller gate

The first entangling gate for trapped ions was proposed by J. I. Cirac and P. Zoller in 1995. In this gate scheme, they consider a linear chain of N ions, all coupled to a single normal mode of motion. Each ion has three internal states: the two qubit states $|0\rangle_n$ and $|1\rangle_n$, and an auxiliary state $|2\rangle_n$ where the subscript denotes the ion number. They also consider classical laser beams that can drive Rabi oscillations between the qubit state $|0\rangle_n$ and either one of the states $|1\rangle_n$ or $|2\rangle_n$ for each ion, with the appropriate frequency and polarization. It is important that the motional state is initially cooled down to its ground state $|0\rangle_m$ for this protocol to work. When the motion is in the ground state, a red-sideband transition from any ion is suppressed, since no state is available to reduce the number of motional quanta by one.

The gate is accomplished by applying a sequence of laser pulses (Raman pulses in the case of hyperfine qubit states), each pulse to a specific target ion, driving a red-sideband transition. Each pulse is characterized by two parameters: parameter $k = 1$ or 2, indicating the duration of the pulse, and parameter $q = 1$ or 2, indicating whether the transition is driven between the atomic state $|0\rangle_n$ and $|q\rangle_n$. The unitary operator $\hat{U}_n^{k,q}$ that describes the evolution of the n-th qubit is given by

$$\hat{U}_n^{k,q}(\phi) = \exp\left[-ik\frac{\pi}{2}(|q\rangle_n \langle 0| \, ae^{-i\phi} + h.c.)\right], \tag{11.8}$$

where $\phi = \arg(\Omega)$ is the phase of the laser beam driving the transition. Since the motion is initially prepared in the ground state, this operation does not alter the state $|0\rangle_n |0\rangle_m$. It induces the following evolution for the states $|0\rangle_n |1\rangle_m$ and $|q\rangle_n |0\rangle_m$;

$$|0\rangle_n |1\rangle_m \quad \rightarrow \quad \cos(k\pi/2) |0\rangle_n |1\rangle_m - ie^{i\phi}\sin(k\pi/2) |q\rangle_n |0\rangle_m, \tag{11.9}$$

$$|q\rangle_n |0\rangle_m \quad \rightarrow \quad \cos(k\pi/2) |q\rangle_n |0\rangle_m - ie^{-i\phi}\sin(k\pi/2) |0\rangle_n |1\rangle_m. \tag{11.10}$$

Specifically, we note that for $k = 1$, the state transformation is given by

$$|0\rangle_n |1\rangle_m \quad \rightarrow \quad -ie^{i\phi} |q\rangle_n |0\rangle_m, \tag{11.11}$$

$$|q\rangle_n |0\rangle_m \quad \rightarrow \quad -ie^{-i\phi} |0\rangle_n |1\rangle_m, \tag{11.12}$$

and for $k = 2$, the states pick up a negative sign

$$|0\rangle_n |1\rangle_m \quad \rightarrow \quad -|0\rangle_n |1\rangle_m, \tag{11.13}$$

$$|q\rangle_n |0\rangle_m \quad \rightarrow \quad -|q\rangle_n |0\rangle_m. \tag{11.14}$$

For all practical purposes, we can set the laser phase $\phi = 0$ to achieve the Cirac-Zoller gate, although maintaining the phase coherence of the optical fields at the location of the ions throughout the computation can be a non-trivial experimental challenge.

The Cirac-Zoller gate can accomplish C^N-Z gate, where the phase of the target qubit is flipped if N control ions are all in the state $|1\rangle$. By applying a Hadamard gate achieving the unitary transformation

$$H = \frac{1}{\sqrt{2}} \begin{pmatrix} 1 & 1 \\ 1 & -1 \end{pmatrix} \tag{11.15}$$

on either side of the target qubit, the Z gate can be converted to a X gate by noting that

$$HZH = \frac{1}{2} \begin{pmatrix} 1 & 1 \\ 1 & -1 \end{pmatrix} \begin{pmatrix} 1 & 0 \\ 0 & -1 \end{pmatrix} \begin{pmatrix} 1 & 1 \\ 1 & -1 \end{pmatrix} = \begin{pmatrix} 0 & 1 \\ 1 & 0 \end{pmatrix} = X. \tag{11.16}$$

Therefore, with the help of two Hadamard gates, the Cirac-Zoller gate can be used to implement a C^N-NOT gate with arbitrary number of control qubits.

As the simplest example, we consider the C-Z gate, where the phase of the target qubit is flipped if the control qubit is in $|1\rangle$ state. This gate consists of three laser pulses $\hat{U}_{l,n} \equiv \hat{U}_l^{1,1} \hat{U}_n^{2,2} \hat{U}_l^{1,1}$, where l-th qubit is the control qubit and n-th qubit is the target qubit. The first unitary operation excites the motional state from $|0\rangle_m$ to $|1\rangle_m$ state, picks up a phase of $-i$, and puts the control qubit in the $|0\rangle_l$ state if and only if the l-th qubit is in $|1\rangle_l$ state. As a result, the l-th qubit is put in the $|0\rangle_l$ state, while the quantum information is transferred to the motional state of the ion chain. The second pulse picks up an overall phase of -1 only if the target qubit is in $|0\rangle_n$ state and the motional state is in $|1\rangle_m$ state (which in turn, originated if the control qubit was in the $|1\rangle_l$ state). The final pulse is used to repeat (or undo) the effect of the first pulse: the motional state is de-excited to $|0\rangle_m$, the control qubit is put back to the $|1\rangle_l$ state, and picks up a phase of $-i$ if the control qubit was originally in the $|1\rangle_l$ state. The time evolution of the state can be expressed as follows:

$$
\begin{array}{ccccccc}
 & \hat{U}_l^{1,1} & & \hat{U}_n^{2,2} & & \hat{U}_l^{1,1} & \\
|0\rangle_l |0\rangle_n |0\rangle_m & \longrightarrow & |0\rangle_l |0\rangle_n |0\rangle_m & \longrightarrow & |0\rangle_l |0\rangle_n |0\rangle_m & \longrightarrow & |0\rangle_l |0\rangle_n |0\rangle_m \\
|0\rangle_l |1\rangle_n |0\rangle_m & \longrightarrow & |0\rangle_l |1\rangle_n |0\rangle_m & \longrightarrow & |0\rangle_l |1\rangle_n |0\rangle_m & \longrightarrow & |0\rangle_l |1\rangle_n |0\rangle_m \\
|1\rangle_l |0\rangle_n |0\rangle_m & \longrightarrow & -i |0\rangle_l |0\rangle_n |1\rangle_m & \longrightarrow & i |0\rangle_l |0\rangle_n |1\rangle_m & \longrightarrow & |1\rangle_l |0\rangle_n |0\rangle_m \\
|1\rangle_l |1\rangle_n |0\rangle_m & \longrightarrow & -i |0\rangle_l |1\rangle_n |1\rangle_m & \longrightarrow & -i |0\rangle_l |1\rangle_n |1\rangle_m & \longrightarrow & -|1\rangle_l |1\rangle_n |0\rangle_m
\end{array}
\tag{11.17}
$$

From this we see that the original states are fully restored at the end of the process, except that an overall -1 sign is picked up when both qubits are in $|1\rangle_j$ (for $j = l, n$) state. This is indeed implements the C-Z gate.

In an extension of this scheme, one can introduce more control qubits in the system. For example, for a C^2-Z gate with two control qubits, one can consider the pulse sequence $\hat{U}_l^{1,1} \hat{U}_k^{1,2} \hat{U}_n^{2,2} \hat{U}_k^{1,2} \hat{U}_l^{1,1}$, where the l-th and k-th qubits act as control qubits, and n-th qubit act as a target qubit. In this sequence, the first gate acts exactly like the one in the case of the C-Z gate. When the second pulse is applied, the motional excitation, if it exists, will be "absorbed" by the k-th qubit if the k-th qubit was in the $|0\rangle_k$ state, but remains if the k-th qubit was in the $|1\rangle_k$ state. This means that the target qubit will only see the motional

excitation if *both* control qubits are in the $|1\rangle_j$ state (for $j = l, k$). The last two pulses simply reverse the effect of the first two pulses, putting all the control qubits and the motional qubit in its original state. As a consequence, the overall phase of -1 is picked up if and only if both control qubits and the target qubit are all in $|1\rangle_j$ state (for $j = l, k, n$).

This procedure can be extended to N control qubits. When the first pulse is applied, the motional mode is excited with one motional quanta if the first control qubit is in the $|1\rangle_l$ state. This motional excitation can be "absorbed" by any one of the subsequent control qubits that are in $|0\rangle$ state, and will not reach the middle pulse applied to the target qubit. So, unless all control qubits are in the $|1\rangle$ states, the operation does not pick up an extra -1 phase for the target qubit in $|1\rangle_n$ state. The pulses are applied in reverse order after the middle pulse, to return all control qubits and the motional qubit to their original states. As a consequence, the overall -1 sign is picked up if and only if all qubits (control and target) are in the $|1\rangle_j$ states, realizing the C^N-Z gate.

Cirac-Zoller scheme provides a powerful framework for realizing a non-trivial multi-qubit gate corresponding to a multi-body interaction. However, it requires the motional mode of the ion chain to be cooled down to its ground state, and remain undisturbed for the duration of the gate operation. This turns out to be an experimentally challenging condition, and despite early demonstrations, the experimental groups have migrated to a gate scheme more robust that does not require such stringent control of the motional degree of freedom.

11.3.2   Mølmer-Sørensen gate

In 1999, A. Sørensen and K. Mølmer published a paper describing an entangling gate scheme that operates without requiring the motional state to be prepared in the ground state. It considers a pair of laser beams (two pairs, if each Rabi oscillation is driven with Raman process) applied to the pair of ions, as shown in Fig. 11.2. The two tones are detuned to the blue and the red of the carrier resonance by an amount δ. The motional mode frequency is given by ν, as in the previous sections. The dynamics of the system is described by Eq. 11.7, just as in the Cirac-Zoller gate case. We consider the case of applying this gate between two ions with indices i and j, and assume that the Lamb-Dicke parameter and the Rabi frequency of the two ions is the same, $\eta_i = \eta_j = \eta$ and $\Omega_i = \Omega_j = \Omega$.

Given that the two beams are detuned, the only resonant process is the case where both ions are excited from the $|00\rangle$ state to the $|11\rangle$ state bu absorbing one photon from each beam, without any change in the motional state $|n\rangle_m$. The Rabi frequency $\tilde{\Omega}$ for the transition between thse two states $|00n\rangle$ and $|11n\rangle$ can be determined from second-order perturbation theory as

$$\left(\frac{\tilde{\Omega}}{2}\right)^2 = \frac{1}{\hbar^2}|\sum_m \frac{\langle 11n|\hat{H}_{int}|m\rangle \langle m|\hat{H}_{int}|00n\rangle}{E_{00n} + \hbar\omega_k - E_m}|^2, \tag{11.18}$$

where the laser energy $\hbar\omega_k$ is the energy of the laser addressing the ion which is excited in the intermediate state $|m\rangle$. Here, we restrict the intermediate states to the red- and the
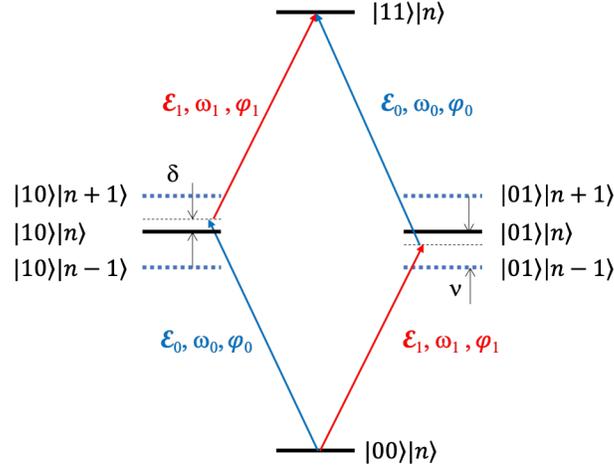
Figure 11.2: Schematic energy level scheme for the Mølmer-Sørensen gate. The motional mode with mode frequency of ν stays in the statistical mixture of $|n\rangle$ states throughout the gate. There are two tones of laser beam applied at ω_0 and ω_1, one detuned to the blue and the other detuned to the red of the single ion carrier transition by an amount δ.

blue-sideband states $|10n+1\rangle$ and $|01n-1\rangle$, and get

$$\tilde{\Omega} = -\frac{(\Omega\eta)^2}{2(\nu-\delta)},$$

(11.19)

where $\delta = \omega_0 - \omega 10$ is the detuning of the laser addressing the first ion. It is remarkable to note that this Rabi frequency is independent of the motional excitation n, as the dependence on n interferes destructively between the two excitation paths and cancels out. This allows us to drive a Rabi oscillation between the $|00\rangle$ and $|11\rangle$ states *independent of* the motional excitation n. When the laser beams are applied for a duration of T, the states evolve under the conditions

$$|00\rangle \longrightarrow \cos\left(\frac{\tilde{\Omega}T}{2}\right)|00\rangle + i\sin\left(\frac{\tilde{\Omega}T}{2}\right)|11\rangle,$$

(11.20)

$$|11\rangle \longrightarrow \cos\left(\frac{\tilde{\Omega}T}{2}\right)|11\rangle + i\sin\left(\frac{\tilde{\Omega}T}{2}\right)|00\rangle,$$

(11.21)

$$|01\rangle \longrightarrow \cos\left(\frac{\tilde{\Omega}T}{2}\right)|01\rangle - i\sin\left(\frac{\tilde{\Omega}T}{2}\right)|10\rangle,$$

(11.22)

$$|10\rangle \longrightarrow \cos\left(\frac{\tilde{\Omega}T}{2}\right)|10\rangle - i\sin\left(\frac{\tilde{\Omega}T}{2}\right)|01\rangle.$$

(11.23)

By controlling the duration of the time evolution to be $\tilde{\Omega}T = \pi/2$, one can start from the

initial state $|00\rangle$ and end up in the maximally-entangled state $(|00\rangle + i\,|11\rangle)/\sqrt{2}$, which is sufficient to function as a universal two-qubit gate.

One can also show that this time evolution is robust against heating, *i.e.*, chance of the motional quanta at random times in the middle of the gate operation.